

Automatic Bone Segmentation for Shoulder MRI using Statistical Shape Models

Zhengyi Yang¹, Jurgen Fripp², Craig Engstrom¹, Shekhar Chandra², Ying Xia², Anthony Paproki², Mark Strudwick¹, Ales Neubert², and Stuart Crozier¹

¹University of Queensland, Brisbane, Queensland, Australia, ²CSIRO, Brisbane, Queensland, Australia

Introduction: Magnetic Resonance Imaging (MRI) can provide exquisite soft tissue discrimination leading to detailed evaluation of shoulder pathology involving structures such as the rotator cuff, biceps tendon, joint cartilages and glenoid labrum [1]. Shoulder MRI has become a central diagnostic tool in patients with shoulder pain and impaired mobility, particularly when clinical diagnosis is difficult. In conditions such as shoulder osteoarthritis and impingement syndrome, it is important to evaluate the morphology of the glenohumeral cartilages, which may be quantitatively analyzed with image segmentation methods. However, direct automatic cartilage segmentation from MR images is challenging due to the relatively thin joint cartilages, high anatomical variance across subjects and potential degenerative conditions associated with morphological changes and intensity inhomogeneity. An approach using bone segmentation as a precursor [2] to subsequent cartilage segmentation [3] has been successfully applied to knee cartilage segmentation, but its feasibility for the glenohumeral joint has not been established. We present a fully automatic shoulder bone segmentation method as a foundation for subsequent automatic cartilage segmentation.

Subjects and Methods: Twenty-five healthy subjects (12 females, 33.6±9.1 years-old, 70.3±11.9 kg) were imaged unilaterally (right shoulder) with a dedicated shoulder coil using a TrueFISP sequence on a 3T Trio Siemens scanner. The medical research ethics committee of the University of Queensland approved the study. Imaging parameters used were: TR/TE=9.23/3.99 ms, field of view (FOV) 140x140 mm² with image dimensions of 640x640x160 and voxel size of 0.2188x0.2188x0.47 mm³. The image datasets were anonymized and no exclusion criteria based on age or gender were used. For each image, the contours of humerus and scapula were manually segmented on each slice (160 slices) by ZY, with expert guidance from CE using ITK-SNAP [4]. To deal with the problem of weak or missing bone boundaries by incorporating shape priors, Active Shape Model (ASM) based segmentation was employed. Separate statistical shape models (SSMs) of humeral and scapular bone elements of the glenohumeral region, along with a combined SSM maintaining the spatial relationship between them, were constructed from manual segmentations. As shown in Figure 1, the pipeline consists of three streamlined modules: preprocessing, initialization, and ASM-based bone segmentation. In preprocessing, the N4 algorithm was used for bias correction and median filtering for smoothing. The SSMs were then initialized by propagating an atlas surface through intensity based registration. In ASM-based segmentation, the combined SSM and separate SSMs were used sequentially. Finally, surface relaxation without shape constraint was carried out to reduce local inaccuracy in segmentation. Taking manual segmentation as ‘ground truth’, volume overlap quantified using the Dice Similarity Coefficient (DSC) was calculated to validate the results.

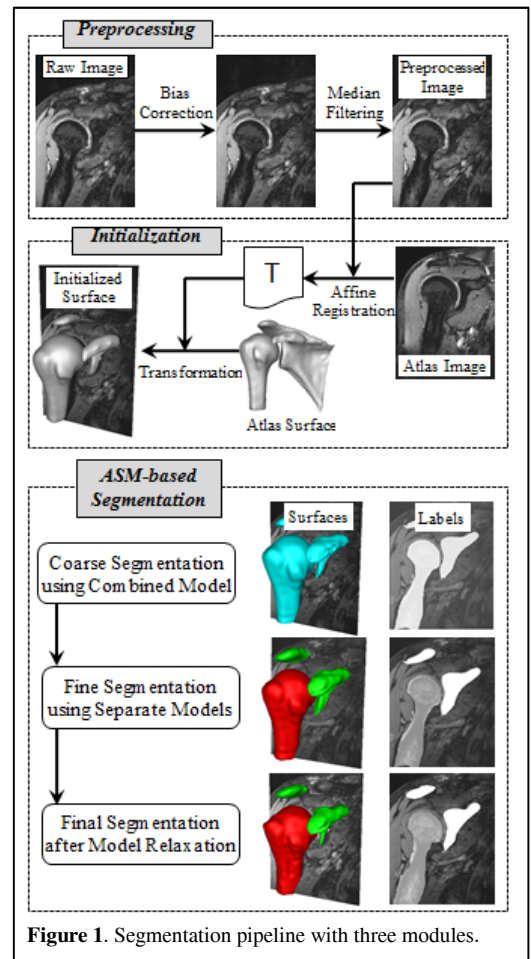


Figure 1. Segmentation pipeline with three modules.

Table I. The DSC of bone segmentation result.

Step	Bone	DSC
ASM	Humerus	0.9282±0.07318
	Scapula	0.7593±0.1319
Relaxation	Humerus	0.9394±0.06956
	Scapula	0.7634±0.1339

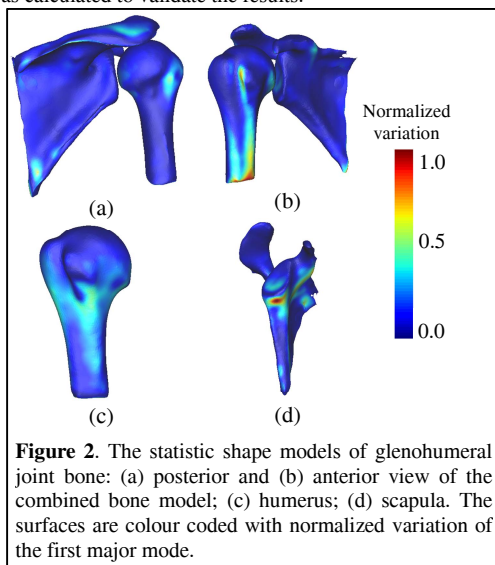


Figure 2. The statistic shape models of glenohumeral joint bone: (a) posterior and (b) anterior view of the combined bone model; (c) humerus; (d) scapula. The surfaces are colour coded with normalized variation of the first major mode.

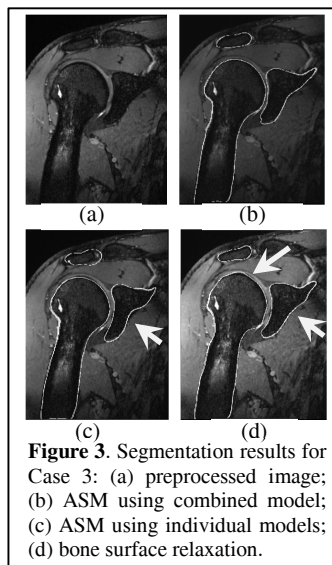


Figure 3. Segmentation results for Case 3: (a) preprocessed image; (b) ASM using combined model; (c) ASM using individual models; (d) bone surface relaxation.

Results and Discussion: As illustrated in Figure 2, the two separate surfaces of the humerus and scapula have 8,000 and 12,000 points, 15,988 and 24,024 triangles, respectively. With the first 5 modes, the humeral, scapular and the combined SSMs can represent 85%, 65%, and 79% variations of the shapes, respectively. We used the first 13, 18, and 11 eigenvalues to account for 95% of variations in the three models, respectively. As indicated by the arrows in Figure 3, after relaxation, the bone boundaries were fine-tuned locally to recover some under- or over-segmentation. Table I shows the DSC achieved before and after surface relaxation and the DSC was significantly improved by relaxation (paired *t*-test, *p* < 0.01). The scapula segmentation was poorer than that of humerus, mainly due to its large variation in shape.

Conclusion: In this study, a fully automatic segmentation pipeline based on shape models for the bone elements of the shoulder was established. The mean DSC between automatic and manual segmentation was 0.94 and 0.76 for the humerus and scapula, respectively. These promising results suggest a high likelihood of the proposed pipeline being integrated into a fully automatic solution for shoulder cartilage segmentation and quantitative analysis of cartilage morphometry.

References:

- [1] E. N. Vinson, *et al.*, AJR, vol. 199, pp. 534-545, 2012.
- [2] J. Fripp, *et al.*, Physics in Medicine and Biology, vol. 52, p. 1617, 2007.
- [3] J. Fripp, *et al.*, IEEE TMI, vol. 29, pp. 55-64, 2010.
- [4] P. A. Yushkevich, *et al.*, Neuroimage, vol. 31, pp. 1116-28, Jul 1 2006.